ACTA NEUROBIOLOGIAE EXPERIMENTALIS

Research paper Acta Neurobiol Exp 2012, 72: 351–364

Effect of dopamine receptor stimulation on voltage-dependent fast-inactivating Na^+ currents in medial prefrontal cortex (mPFC) pyramidal neurons in adult rats

Bartłomiej Szulczyk, Aneta Książek, Wioleta Ładno, and Paweł Szulczyk*

Department of Physiology and Pathophysiology, Medical University of Warsaw, Warsaw, Poland
*Email: pawel.szulczyk@wum.edu.pl

Impaired working memory is a common feature of neuropsychiatric disorders. It is dependent on control of the medial prefrontal cortex (mPFC) neurons by dopamine. The purpose of this study was to test the effects of a $D_{1/5}$-type dopamine receptor agonist (SKF 38393, 10 μM) on the membrane potential and on voltage-dependent fast-inactivating Na^+ currents in mPFC pyramidal neurons obtained from adult (9-week-old) rats. Treatment of the pyramidal neurons with SKF 38393 did not affect the membrane potential recorded with the perforated-patch method. When recordings were performed in cell-attached configuration, the application of SKF 38393 did not change the Na^+ current amplitude and shifted the current-voltage relationship of the Na^+ currents towards hyperpolarisation, thus resulting in an increase of the current amplitudes in response to suprathreshold depolarisations. Pretreatment of the cells with a $D_{1/5}$ receptor antagonist (SCH 23390, 10 μM) abolished the effect of the $D_{1/5}$-type receptors on Na^+ currents. The effect of the $D_{1/5}$ agonist was replicated by treating the cells with a membrane-permeable analogue, cAMP (8-bromo-cAMP, 100 μM), and the effect was blocked by treating the cells with a protein kinase A inhibitor, (H-89, 2 μM). In recordings performed from mechanically and enzymatically dispersed pyramidal neurons in the whole-cell configuration, when the cell interior was dialysed with pipette solution, application of the $D_{1/5}$ agonist decreased the Na^+ current amplitude without changing the current-voltage relationship. We conclude that in the mPFC pyramidal neurons in slices with an intact intracellular environment (recordings in the cell-attached configuration), the activation of $D_{1/5}$ dopamine receptors increases the fast-inactivating Na^+ current availability in response to suprathreshold depolarisations. The maximum Na^+ current amplitude was not changed. A cAMP/protein kinase A pathway was responsible for the signal transduction from the $D_{1/5}$ dopamine receptors to the Na^+ channels.

Key words: mPFC, pyramidal neurons, $D_{1/5}$ dopamine receptors, Na^+ currents, membrane potential, cAMP, PKA, cell-attached, perforated patches, whole cell, rats

INTRODUCTION

Proper functioning of the prefrontal cortex is compromised during natural aging and in certain neuropsychiatric disorders, including dementia, attention deficit hyperactivity disorder, drug addiction, schizophrenia and traumatic brain injury. A common feature of these pathologies is impairment of the working memory (Williams and Castner 2006, Dash et al. 2007, Zohar et al. 2011), which is the process of storing information for a short period of time and using it to guide future behaviours (Baddeley and Hitch 1974). Regulation of pyramidal neuron activity by the dopamine receptors is considered to be a fundamental aspect of the working memory (Goldman-Rakic 1995, Sobotka et al. 2005, Nowak et al. 2012).

For these reasons it is important to determine the mechanism underlying the dopaminergic control of prefrontal cortex pyramidal neuron activity. This activity is produced by an ensemble of ionic channels, including voltage-gated Na^+ channels.

There are 2 types of voltage-dependent Na^+ currents in the cortical neurons: fast-inactivating Na^+ currents and persistent Na^+ currents. The fast-inactivating currents are large amplitude Na^+ currents undergoing steady-state and time-dependent inactivation (e.g.

Correspondence should be addressed to P. Szulczyk
Email: pawel.szulczyk@wum.edu.pl

Received 15 October 2012, accepted 31 December 2012

© 2012 by Polish Neuroscience Society - PTBUN, Nencki Institute of Experimental Biology

Maurice et al. 2001, Witkowski and Szulczyk 2006). In contrast, persistent Na^+ currents have a small amplitude, undergo little inactivation during sustained membrane depolarisation and are weakly time-dependently inactivated (Crill 1996).

Five subtypes of G-protein-coupled dopamine receptors exist. These receptors are grouped into the following two categories: (1) $D_{1/5}$-type, which includes D_1 and D_5 type receptors, and (2) $D_{2/4}$ type, which includes the D_2, D_3 and D_4 type receptors that control cellular effectors by different transduction systems (for a review see Beaulieu and Gainetdinov 2011).

Previous studies have shown that dopamine or $D_{1/5}$-type receptor activation increases the excitability and activity of mPFC pyramidal neurons in rats without changing the action potential amplitude (Penit-Soria et al. 1987, Yang and Seamans 1996, Shi et al. 1997, Gorelova and Yang 2000, Henze et al. 2000, Lavin and Grace 2001, Tseng and O'Donnell 2004, Chen et al. 2007, Thurley et al. 2008, Moore et al. 2011).

Several studies were conducted to elucidate the mechanisms involved in the dopamine- dependent increase in pyramidal neuron activity in mPFC. It was demonstrated that dopamine upregulates the NMDA receptors (Seamans et al. 2001, Gonzalez-Islas and Hablitz 2003, Chen et al. 2004, Tseng and O'Donnell 2005, Kruse et al. 2009), activates voltage-dependent Ca^{++} currents (Heng et al. 2011), activates persistent Na^+ currents (Gorelova and Yang 2000, Maurice et al. 2001) and suppresses voltage-dependent ID-type K^+ currents (Dong and White 2003). All of these mechanisms should lead to an increase in pyramidal neuron activity. One exception was the effect of $D_{1/5}$ dopamine receptor activation on fast-inactivating Na^+ currents. Previous studies have consistently shown that the stimulation of $D_{1/5}$ dopamine receptors decreases the amplitude of the fast-inactivating Na^+ current when recorded in the whole-cell configuration from the dispersed pyramidal neurons obtained from younger rats (Maurice et al. 2001, Carr et al. 2003, Peterson et al. 2006), which suggests that this type of stimulation opposes a dopamine-dependent increase in pyramidal neuron activity.

The aim of this study was to elucidate the function of the $D_{1/5}$ dopamine receptors in regulating the voltage-dependent and fast-inactivating Na^+ currents in mPFC pyramidal neurons.

METHODS

The experimental procedures used in this study adhered to the institutional and international guidelines on the ethical use of animals and of the local ethical committee (II Local Ethical Committee, Decision 1/2009). The experiments were performed on the neurons of adult (60–65-day-old) male rats (WAG Cmd; Spear 2000) obtained from a local animal house. Brain slices were prepared as previously described (Witkowski and Szulczyk 2006, Witkowski et al. 2008). After the induction of deep anaesthesia by ethylum chloratum, the brains were removed and placed in a cold (0–4°C), oxygenated extracellular solution composed of the following compounds (in mM): sucrose (234), KCl (2.5), NaH_2PO_4 (1), glucose (11), $MgSO_4$ (4), N-(hydroxyethyl)piperazine-N-(2-ethanesulfonic acid)-Cl (HEPES-Cl; 15) and $CaCl_2$ (0.1). The pH was adjusted to 7.4 with N-methyl-D-glucamine and the osmolality was 330 mOsm/kg H_2O. Coronal slices (300-μm-thick) were prepared from the cerebral prefrontal tissue using a vibratome (Vibratome 1000, Pelco International, CA, USA).

Recordings from the pyramidal neurons in slices

The slices were incubated for 40 min in a warm (34°C) extracellular solution infused with 95% O_2 and 5% CO_2 and containing the following compounds (in mM): NaCl (130), KCl (2.5), glucose (10), $NaHCO_3$ (25), NaH_2PO_4 (1.25), $MgCl_2$ (2) and $CaCl_2$ (2) at a pH of 7.4 and an osmolality of 320 mOsm/kg H_2O. During the recordings the slices were perfused with the same extracellular solution containing blockers of GABAergic and glutaminergic transmission (50 μM picrotoxin, 10 μM DNQX and 50 μM AP-4).

The slices were placed in a bath chamber (RC-24E, Warner Instruments, LLC, MA, USA) on the stage of an upright Nikon microscope (Eclipse E600FN; Nikon Instech Co., Ltd., Japan) and maintained at room temperature. Images of neurons were recorded using infrared-differential interference contrast microscopy with a 40× water immersion objective, a camera (C7500-50) and a camera controller (C2741-62) from Hamamatsu Photonics K.K. (Japan). The recordings were obtained from layer V pyramidal neurons in the infralimbic and prelimbic mPFC at a depth of 600–800 μm from the cortical surface. The recordings were obtained using

Multiclamp 700A and Digidata 1332A software (pClamp 9.0, Molecular Devices, CA, USA).

To test the effect of the $D_{1/5}$ agonist on the membrane potential, the membrane potentials were recorded under current-clamp conditions in the gramicidin perforated-patch recording mode (Akaikke and Harata 1994). The pipette solution contained the following compounds (in mM): potassium gluconate (105), KCl (20), HEPES-Na^+ (10), ethylene glycol-bis-(2-aminoethylether)-N,N,N′,N′-tetraacetic acid (0.1) and gramicidin (10 μg/ml) at a pH of 7.25 and an osmolality of 280 mOsm/kg H_2O. Progress during membrane perforation was monitored by observing a slow gradual decrease in access resistance. After 20 min the access resistance reached a steady level of 15–20 MΩ. After stable electrical access to the cell was obtained, the membrane potential was continuously recorded for 10 min for the control, 10 min with the tested compounds present and 10 min after washout of the compounds. Access resistance was periodically inspected and the recording was discarded if the resistance rapidly decreased. The membrane potential recordings were digitised at 20 kHz.

The voltage-dependent Na^+ currents were recorded from macropatches after formation of a GΩ seal in the cell-attached configuration. The pipette solution contained the following compounds (in mM): NaCl (120), KCl (5), $CaCl_2$ (2), $MgCl_2$ (2), HEPES (10), 4-aminopiridine (4-AP; 5) and tetraethylammonium chloride (TEA-Cl; 30) at a pH of 7.4 and an osmolality of 300 mOsm/kg H_2O. The pipette open-tip resistance was 10–12 MΩ. The cell-attached patch recordings were filtered at 10 kHz (eight-pole Bessel filter) and sampled at 100 kHz. In cells in which the patch Na^+ current recording was performed, the membrane potential was measured in the current-clamp configuration after the data were collected in the cell-attached configuration and the patch was ruptured. Access resistance was 15–20 MΩ. All of the voltage levels used in the cell-attached configuration were applied relative to this membrane potential value in each individual cell.

The pipettes were fabricated from borosilicate glass capillaries (O.D. 1.5 mm, I.D. 0.86 mm; Harvard Apparatus, Edenbridge, UK) using a P-97 puller (Sutter Instruments, Inc., CA, USA) and were coated with Sylguard. The junction potential was zeroed when the pipette tip was immersed in the bath.

The relationship between the voltage and normalised current (voltage-current relationship) was fitted to a sigmoid curve using Clampfit 10 software (Molecular Devices, CA, USA).

The perfusion rate of the recording chamber (2 ml/min) was controlled using a VC-6 valve controller (Warner Instruments, LLC, USA).

Recordings from dissociated pyramidal neurons

Slices were placed in an extracellular solution containing the following compounds (in mM): NaCl (118), KCl (5.3), $CaCl_2$ (1.8), $MgSO_4$ (0.4), $NaHCO_3$ (26), NaH_2PO_4 (0.9), kynurenic acid (1), N-nitro-L-arginine (0.1) and pyruvic acid (0.2), pH 7.4, with an osmolality of 310 mOsm/l. The solution was infused with 95% O_2 and 5% CO_2. The slices were stored until use at a temperature of 21–23°C .

Portions of slices that were 2.2–3.5 mm anterior to the Bregma, 3–5 mm below the upper cortical surface and 0.1–0.9 mm from the midline (Kolb 1984, Berger et al. 1991) were dissected and transferred to a solution infused with O_2 and containing the following reagents (in mM): NaCl (135), HEPES-Cl (10), KCl (5), $MgSO_4$ (1), $CaCl_2$ (1.8), glucose (10) and 1 mg/ml of protease type XIV (Sigma Aldrich, St Louis, USA) at pH 7.4 (adjusted with NaOH) and an osmolality of 300 mOsm/l. The enzymatic breakdown was allowed to proceed for 18 min at 32°C. To stop the enzymatic activity, the slices were washed three times with the same solution but without the enzyme. Portions of the slices were mechanically dissociated using Pasteur pipettes that progressively decreased in diameter. The dissociated neurons were transferred to the recording chamber (type RC-27N, Warner Instruments LLC, USA) under an Olympus inverted microscope (Olympus Co., Tokyo, Japan). Cells were identified under DIC optics (magnification 400×) according to previously established criteria. The pyramidal neurons selected for current recordings had a smooth three-dimensional appearance, a triangular shape, residual apical and basal dendrites and a short axon at the base (Fig. 1B in Witkowski and Szulczyk 2006, Witkowski et al. 2008).

Initially, the cells were perfused with an extracellular solution containing the following ingredients (in mM): NaCl (130), KCl (5), $MgCl_2$ (2), $CaCl_2$ (2), glucose (12) and HEPES-Cl (10). The pH was adjusted to 7.4 with NaOH, and the osmolality was 320 mOsmol/kg.

After a cell was identified, the extracellular solution was replaced with a solution designed to isolate the Na^+ current. This solution contained the following ingredients (in mM): NaCl (25), TEA-Cl (tetraethylammonium chloride) (30), choline chloride (90), HEPES-Cl (10), $MgCl_2$ (2), $CaCl_2$ (1) and glucose (15) (the pH was adjusted to 7.4 with TEA-OH, and the osmolality was 340 mOsmol/kg). The intracellular solution designed to isolate the Na^+ current contained the following ingredients (in mM): Cs-methanesulphonate (95), NaCl (15), EGTA (ethylene-glycol-bis(β-aminoethylether)-N,N,N',N'- tetraacetic acid) (11), HEPES-Cl (10), $CaCl_2$ (2), Mg-ATP (Mg adenosine triphosphate) (2), Na_3GTP (Na_3 guanosine 5'-triphosphate) (0.4), phosphocreatine (12), and leupeptin (0.01, osmolarity 280 with sucrose, the pH adjusted to 7.2 with CsOH). K^+ ions were excluded from the intracellular and extracellular solutions. To block the voltage-dependent Ca^{++} currents, 0.5 μM $LaCl_3$, 100 μM $CdCl_2$ and 50 μM $NiCl_2$ were added to the extracellular solution.

The voltage-clamp recordings were obtained in a whole-cell configuration using an Axopatch 1D amplifier at room temperature (21–23°C). pClamp software was used (Molecular Devices, USA). Pipettes were fabricated from borosilicate glass capillaries (O.D. 1.5 mm, I.D. 0.86 mm; Harvard Apparatus, Edenbridge, UK) using a P-87 puller (Sutter Instruments, Inc., Novato, CA, USA) and were then fire-polished. The junction potential was nulled with the pipette tip immersed in the bath. Patch pipettes were sealed against the cell membrane and the membrane was ruptured spontaneously or by suction. The electrode capacitance was compensated by the circuit of the amplifier. Access resistance ranged from 5–7 MΩ. The following steps were taken to eliminate any significant voltage clamp error: (1) a series resistance compensation of 80% was routinely applied; (2) the concentration of the Na^+ ions in the extracellular solution was decreased to 25 mM (the concentration gradient for Na^+ ions was 25/15 mM); (3) for each cell, the I/V relationship was tested and the reversal potential was estimated. Cells with signs of inadequate voltage control (discontinuities in the current-voltage relationship, Isaac and Wheal 1993) were excluded; (4) Only cells with residual processes were chosen. In order to subtract the (passive) leak and capacitive transient from the total current evoked by command pulses when recording the Na^+ currents in the whole-cell configuration, a P/4 protocol was applied. A series of 4 scaled-down versions of the command waveform was generated, the responses were measured, accumulated and subtracted from the data. The procedure was performed by pClamp 10 software (compare Bezanilla and Armstrong 1977).

Chemical compounds were delivered to the cell in the extracellular solution through a gravity-fed large pore pipette that was held approximately 200–300 μm from the cell (EVH-9, Biologic Science Instruments, Claix, France). SKF-38393 hydrobromide was purchased from Tocris Cookson (Bristol UK, Cat. No. 0922), dissolved in deionised water, stored as frozen aliquots at −25°C and diluted to a 10 μm concentration in the artificial extracellular solution immediately before application. Other chemical compounds were obtained from Polskie Odczynniki Chemiczne (Poland), Sigma-Aldrich (Poland) and Ascent Scientific (UK).

All of the results presented in this paper are shown as the mean ± SEM. GraphPad InStat software v3.06 (GraphPad Software, Inc., CA, USA) was used for the statistical analyses.

RESULTS

Control of membrane potential by $D_{1/5}$ dopamine receptors

Treatment of pyramidal neurons with a $D_{1/5}$ agonist (SKF-38393, 10 μM) did not affect the membrane potential in any of the individual neurons tested as measured by perforated-patch recordings (Fig. 1A). The average membrane potential was −64.9 ± 0.8 mV (n=8) during the control recording, −65.2 ± 0.9 mV (n=8) at the end of a 10-min agonist treatment and −65.0 ± 0.2 mV (n=5) after a 10-min washout period (Kruskal-Wallis test, KW=0.029, P=0.986). We concluded that activation of the $D_{1/5}$ dopamine receptors does not affect the membrane potential in mPFC pyramidal neurons.

Control of the fast-inactivating Na^+ currents recorded in the cell-attached configuration by $D_{1/5}$ dopamine receptors

To record fast-inactivating Na^+ currents, rectangular voltage steps in 10-mV increments from 0 mV to −90 mV, every 2 seconds and lasting 7 ms, were applied to the pipette. These voltage steps changed the patch

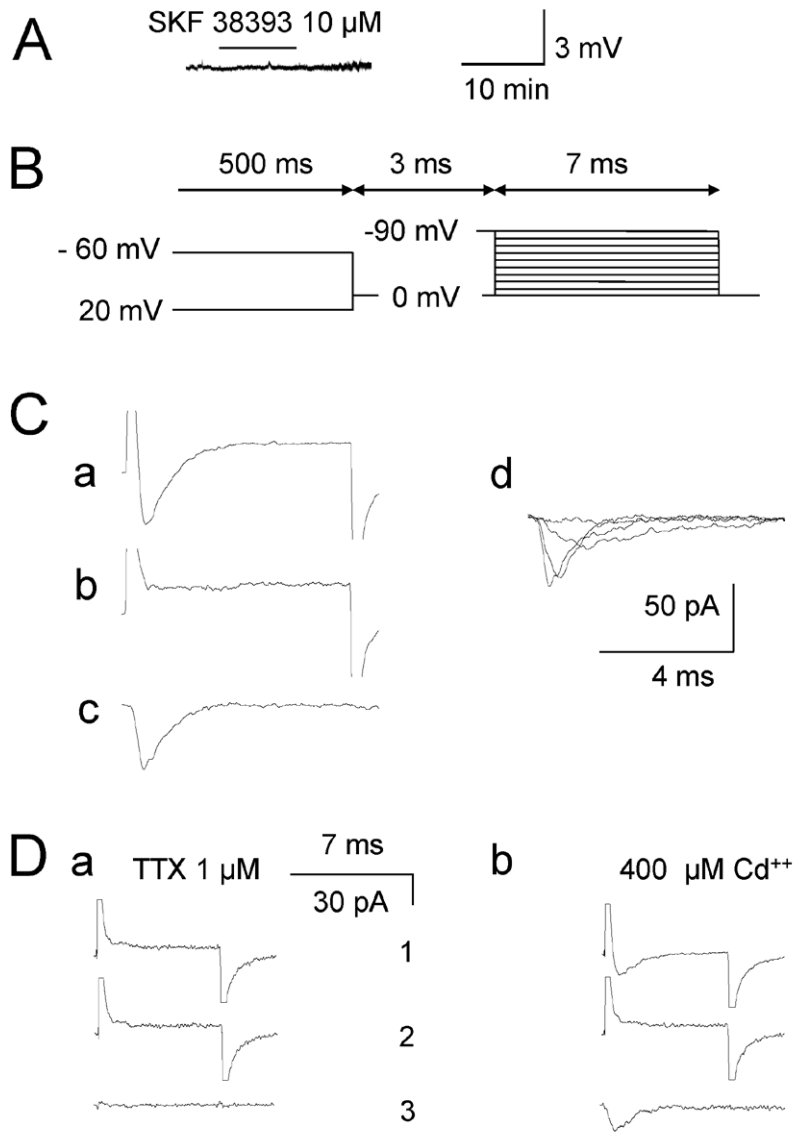

Fig. 1. Effect of a D1 receptor agonist on the membrane potential. Na^+ patch current recording method. (A) The original recording of the membrane potential is shown. The black horizontal line indicates the 10-min SKF 38393 (10 µM) treatment. (B) The voltage protocol used to isolate the voltage-dependent Na^+ current in the cell-attached configuration is shown. Na^+ currents were induced with 7-ms rectangular voltage steps from 0 to −90 mV applied to the patch pipette in 10 mV increments. Therefore, the patch membrane potential was adjusted from its resting value to +90 mV above the resting membrane potential in 10 mV increments. The voltage steps were preceded by a pre-pulse of −60 mV or +20 mV applied to the pipette and lasting 500 ms. Therefore, the patch membrane potential was kept at +60 mV above or 20 mV below the resting membrane potential for 500 ms. Between the pre-pulse and voltage steps, the membrane potential was maintained at the resting membrane potential for 3 ms. (C) (a) The capacitance transient and Na^+ current induced by a voltage step depolarisation to −5 mV that was preceded by a −85 mV pre-pulse lasting 500 ms are shown. (b) The capacitance transient induced by a voltage step to −5 mV that was preceded by a −5 mV pre-pulse lasting 500 ms is shown. (c) An Na^+ current trace obtained by subtracting the current displayed in "b" from the current displayed in "a" is shown. (d) An example of Na^+ current traces induced by voltage steps to −25, −15, −5, and +5 mV is shown. (D) (a) The Na^+ current was not induced by a voltage step when 1 µM Tetrodotoxin was present in the pipette solution. (b) The Na^+ current was present when the pipette solution contained 400 µM Cd^{++}. The patch membrane currents were induced by a 7-ms voltage step to −5 mV preceded by a −85-mV hyperpolarisation that lasted 500 ms (1) or a −5-mV depolarisation that lasted 500 ms (2). Current traces after the subtraction calculation are shown (3).

membrane potential to +90 mV above the resting potential in 10-mV increments. This voltage protocol was preceded by a +20-mV or −60-mV pre-pulse applied to the pipette that lasted 500 ms. During the +20-mV pre-pulse, the patch membrane potential dropped to 20 mV below the resting membrane potential, which partially removed the steady-state inactivation of the Na^+ currents in the patched membrane. During the −60-mV pre-pulse, the patch membrane potential increased to +60 mV above the resting membrane potential and the patch Na^+ currents were in a completely inactive steady state. Between the rectangular voltage steps and the pre-pulses, the pipette potential was maintained at 0 mV (the patch was at a resting membrane potential) for 3 ms. Additionally, the patch was at resting membrane potential during the intervals between voltage step applications (Fig. 1B). At the end of the patch Na^+ current recordings, the patch membrane was ruptured and the true membrane potential was measured in current-clamp configuration. The mean membrane potential recorded immediately after the cytoplasm was accessed was −65.6 ± 0.5 mV (n=73), which was comparable to the membrane potential measured during the perforated-patch recordings (see above, −65.9 ± 1.26 mV, n=16, unpaired t test, P=0.8135). All of the applied voltage steps plotted on the horizontal axes in Figures 2Aa and Ca are expressed relative to the potential measured after the cell was ruptured. The true pre-pulse hyperpolarising and depolarising potentials were −85.6 ± 0.5 mV and −5.6 ± 0.5 mV (n=73), respectively. This amount of pre-pulse depolarisation (to −5.6 mV) completely inactivated the fast-inactivating Na^+ currents recorded in both the cell-attached (Magee and Johnston 1995, Rosenkranz and Johnston 2007) as well as whole-cell configurations (Rola et al. 2002, Szulczyk and Szulczyk 2003, Rola and Szulczyk 2004, Witkowski and Szulczyk 2006).

The following procedure was used to isolate the fast-inactivating Na^+ currents: a rectangular voltage step, e.g. to −5 mV, preceded by a −85-mV pre-pulse, was used to induce a large capacitance transient with an inward Na^+ current (Fig. 1Ca). When the pre-pulse amplitude was −5 mV, the same rectangular voltage step induced only a capacitance transient because the Na^+ current was in an inactive steady state (Fig. 1Cb). Subtraction of the trace presented in Figure 1Cb from the trace shown in Figure 1Ca revealed a purely inward fast-inactivating Na^+ current (Fig. 1Cc). The average of 8 to 12 subtracted traces induced by each step was calculated. As a result, Na^+ currents induced by a series of voltage steps were obtained. Traces of Na^+ currents in response to the voltage steps −25, −15, −5 and +5 mV are shown in Figure 1Cd (only 4 traces from the family of Na^+ currents are shown for clarity). The voltage protocol shown in Figure 1B was applied under control conditions, during 5- or 10-min treatment with the test compound and after a 10-min washout period.

Voltage-dependent and fast-inactivating Na^+ currents were detected in 209 patches and were absent in 3 patches. When 1 μM of Tetrodotoxin citrate was added to the pipette solution, Na^+ currents were not detected in the successive recordings from 32 patches (Fig. 1Da). This indicates that only Na^+ currents were recorded in the cell-attached configuration in our study. Furthermore, the currents were not affected by the presence of an inorganic Ca^{++} channel blocker ($CdCl_2$, 400 μM) in the pipette solution (Fig. 1Db). This indicates that the patch currents were not contaminated by voltage-dependent Ca^{++} currents. The pipette solution always contained the K^+ channel blockers 4-AP and TEA-Cl.

The maximum Na^+ current amplitude recorded in the cell-attached configuration was 11.9 ± 1.0 pA (n=147) and was similar to the maximum amplitude of the Na^+ current recorded previously by other authors in the same configuration (Gasparini and Magee 2002, Rosenkranz and Johnston 2007). The maximum amplitude of the Na^+ currents measured at the end of the 7-ms depolarising voltage step was 0.09 ± 0.1 pA (n=147), thus indicating that the recorded voltage-dependent Na+ currents were completely time-dependently inactivated (e.g. Fig. 1 Ccd, Db3, Fig. 2Ba). This demonstrates that all of the Na^+ currents recorded in the cell- attached configuration in this study had a transient nature.

The effects of chemical compounds on Na^+ currents were tested when the Na^+ current amplitude was above 10 pA. Fast-inactivating Na^+ currents were induced using a series of 7-ms depolarising rectangular voltage steps that were applied to the patch membrane (Fig. 1B) in the control conditions during a 5-min SKF 38393 ($D_{1/5}$ receptor agonist; 10 μM) treatment and after a 10-min recovery period, and the resulting Na^+ current-voltage relationship were constructed. During $D_{1/5}$ receptor activation, the Na^+ current-voltage relationship between the threshold and the maximum cur-

rent shifted towards hyperpolarisation and did not recover after the 10-min washout period in all the pyramidal neurons tested (Fig. 2Aa). As a result, the suprathreshold voltage steps to −26 mV and −16 mV induced larger Na^+ currents during and after the $D_{1/5}$ receptor agonist treatment when compared to the control recordings (Fig. 2Ab). However, the maximum Na^+ currents recorded under the control conditions (20.0 ± 5.4 pA, n=12), at the end of the D1 agonist treatment (19.2 ± 5.1 pA, n=12) and at the end of the recovery period (21.0 ± 10.1 pA, n=5) were not significantly different (Kruskal-Wallis test, KW=0.12, P=0.94, Fig. 2Bab). The τ values of the time-dependent inactivation of the maximum Na^+ currents under control conditions, during the SKF 38393 treatment and after the washout were 0.74 ± 0.07 ms (n=14), 0.77 ± 0.10 ms (n=14) and 0.72 ± 0.11 ms (n=5), respectively, and no significant difference was observed among these values (Kruskal-Wallis test, KW=0.18, P=0.91).

To quantify the effect of the $D_{1/5}$ agonist on the Na^+ current-voltage relationship, the currents were normalised to the maximum current recorded under the control conditions, during the $D_{1/5}$ agonist treatment and after the washout period. All of the currents recorded from the threshold to the maximum were fitted to a sigmoid curve (Fig. 2Ca). The normalised currents were measured at the patch membrane potential at which half of the current amplitude under the control conditions was reached. At this membrane potential (dotted vertical line in Fig. 2Ca) Na^+ currents were compared under control conditions, during $D_{1/5}$ agonist treatment and after the washout period in each tested neuron. We found that the current amplitude increased during the agonist treatment (131.1 ± 6.3%, n=14, P<0.001 *versus* control) and did not recover after the washout period (137.2 ± 12.1%, n=5, P<0.01 *versus* control) relative to the control half current amplitude (100%, n=14, Kruskal-Wallis test, KW=18.609, followed by Dunn's test, Fig. 2Cb). This effect was abolished when the $D_{1/5}$ receptor agonist was applied together with the antagonist SCH 23390. The half amplitude of the Na^+ current measured when the $D_{1/5}$ antagonist was applied alone (100%, SCH 23390, 10 μM) did not change when the $D_{1/5}$ agonist (SKF 38393, 10 μM) and $D_{1/5}$ antagonist (100%, SCH 23390, 10 μM) were applied together (105.2%, n=5, Wilcoxon test, P=0.62, Fig. 3A).

Dopamine receptors are linked to the cAMP and protein kinase A intracellular transduction pathway (Beaulieu and Gainetdinov 2011). Therefore, involvement of cAMP and protein kinase A in the regulation of Na^+ currents by D_1 dopamine receptors was investigated. First, the ability of cAMP to affect the membrane potential was tested. A 10-min treatment with a membrane-permeable analogue of cAMP (8-bromo-cAMP, 100 μM) did not change the membrane potential of the pyramidal neurons (recorded using the perforated-patch method, Fig. 3Ba). The membrane potential was −66.1 ± 3.1 mV under the control conditions, −65.5 ± 3.4 mV at the end of the 10-min 8-bromo-cAMP treatment and −65.6 ± 3.6 mV after the 10-min washout period (repeated-measure ANOVA, P>0.05, n=5). Therefore, changes in the Na^+ current during 8-bromo-cAMP treatment cannot be a secondary effect caused by membrane potential fluctuations.

The effect of the 8-bromo-cAMP (100 μM) was also tested on voltage-dependent and fast- inactivating Na^+ currents. The half current amplitude recorded in control conditions (100%) significantly increased during the 8-bromo-cAMP treatment (128.2 ± 4.8%, n=9, P<0.01 *versus* control) and during the washout period (157.6 ± 9.0%, n=5, P<0.001 *versus* control, Kruskal-Wallis Test, KW=18.84, followed by Dunn's test, Fig. 3Bb). There was no difference in the maximum current amplitude recorded under the control conditions (26.6 ± 4.0 pA, n=9), during 8-bromo-cAMP treatment (25.0 ± 3.8 pA, n=9) and after the washout period (21 ± 2.2 pA, n=5, Kruskal-Wallis Test, KW=0.67, P=0.72). The τ values of the time-dependent inactivation of the maximum Na^+ currents under the control conditions, during the 8-bromo-cAMP treatment and after the washout period were 0.70 ± 0.05 ms (n=9), 0.73 ± 0.06 ms (n=9) and 0.66 ± 0.08 ms (n=5), respectively (ANOVA, P=0.73), and these values were not significantly different.

These data suggest that the intracellular second messenger cAMP and $D_{1/5}$ dopamine receptors regulate the voltage-dependent Na^+ currents in pyramidal neurons in a similar manner.

Previously it was shown that the intracellular second messenger cAMP activates different intracellular transduction pathways in addition to protein kinase A, which is its classical effector (Holz et al. 2006). To determine whether the effect of the $D_{1/5}$ agonist on the fast-inactivating Na^+ current recorded in the cell-attached configuration was dependent on protein kinase A activation, brain slices were pre-incubated in the protein kinase A antagonist H-89 (2 μM). In cells treated with H-89, the control current half amplitude (100%) was not significantly influenced by 10 μM of

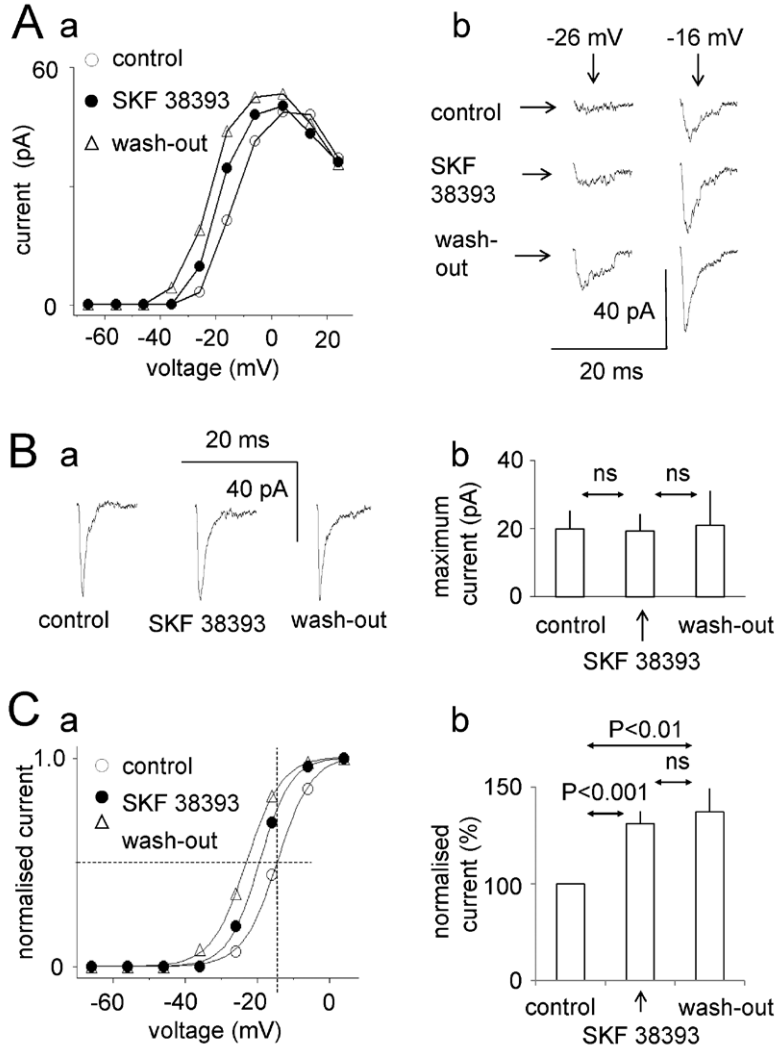

Fig. 2. Effect of SKF 38393 on fast-activating and fast-inactivating Na^+ currents recorded in the cell-attached configuration. (A) (a) The effect of SKF 38393 on the Na^+ current-voltage relationship induced by voltage steps (from −66 mV to +24 mV) under control conditions (open circles, control), at the end of a 5-min 10 μM SKF 38393 treatment (filled circles, SKF 38393) and after the 10-min washout period (open triangles, washout) is shown (horizontal axis – the value of the step depolarisations and vertical axis – evoked current). (b) Examples of the submaximal Na^+ currents induced by voltage steps to −26 mV and −16 mV before (control) and during SKF38393 treatment (SKF38393), as well as after the washout period (washout). (B) (a) Examples of the maximum current recorded in the control condition (control), at the end of 5 min of 10-μM SKF 38393 application (SKF 38393) and after the 10-min recovery (washout) are shown. (b) The average maximum amplitude of the Na^+ patch currents before (control), during (SKF 38393) and after SKF 38393 treatment is shown. (C) (a) Examples of the current-voltage relationship under control conditions (open circles, control), at the end of a 5-min 10-μM SKF 38393 treatment (SKF 38393, filled circles) and after the 10-min recovery period (open triangles, washout) are shown. The currents were normalised to the maximum Na^+ current amplitude recorded under the control conditions, during the D1 agonist treatment and after the washout period. The dotted horizontal line marks the level of the half maximum amplitude of the Na^+ current recorded under the control conditions. The vertical dotted line indicates the membrane potential at which the normalised Na^+ current amplitudes were compared. (b) A comparison of current amplitudes under the control conditions (control), at the end of a 5-min 10-μM SKF 38393 treatment (SKF 38393) and after the 10-min washout period (washout) is shown. The currents were measured at the patch membrane potential at which half of the current amplitude under the control conditions was reached (dotted vertical line in Ca). Relative currents measured during the SKF 38393 treatment and after the washout are expressed in relation to the half current amplitude measured under the control conditions (100%). Results from the same patch are shown in Aa, Ab, Ba and Ca.

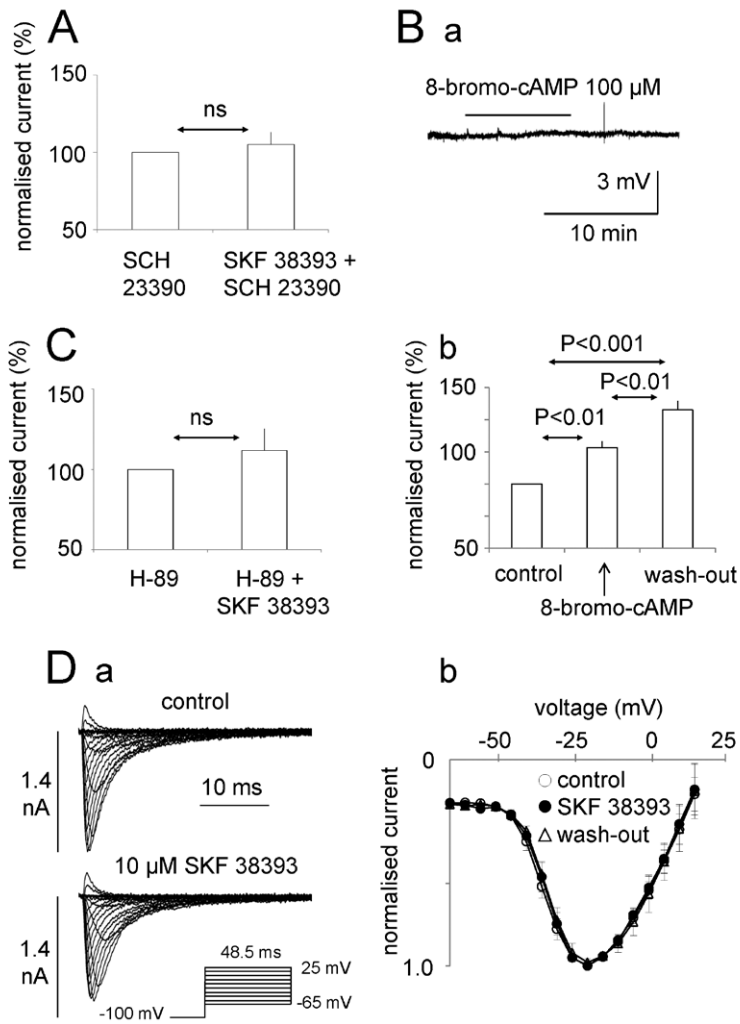

Fig. 3. Effect of SKF 38393, SCH 23390 and 8-bromo-cAMP on fast-activating and fast-inactivating voltage-dependent Na^+ currents recorded in the cell-attached configuration. Effect of SKF 38393 on fast-activating and fast-inactivating Na^+ currents recorded in the whole-cell configuration. (A) A comparison of the current amplitudes measured under the control conditions (SCH 23390) and at the end of a 5-min 10-µM SKF 38393 treatment (SKF 38393 + SCH 23390) are shown. The relative currents measured during the SKF 38393 treatment are expressed in relation to the half current amplitude measured under the control conditions (100%, compare Fig. 2Ca). (B) (a) The effect of a membrane-permeable cAMP analogue (8-bromo-cAMP, 100-µM) on the membrane potential (the black horizontal line marks the 10-min treatment) is shown. (b) A comparison of the current amplitudes measured under control conditions (control), at the end of a 5-min 100-µM 8-bromo-cAMP treatment (8-bromo-cAMP) and after the washout period (washout) is shown. The relative currents measured during the 8-bromo-cAMP treatment and after the 10-min washout period are expressed in relation to the half current amplitude measured under the control conditions (100%, compare Fig. 2Ca). (C) A comparison of current amplitudes under the control conditions (H-89) and at the end of a 5-min 10-µM SKF 38393 treatment (H-89, SKF 38393). Currents were measured at the patch membrane potential at which half of the current amplitude under the control conditions was reached. The relative currents measured during the SKF 38393 treatments were expressed in relation to the half current amplitude measured under the control conditions (100%, compare Fig. 2Ca). (D) (a) The original recordings of the voltage-dependent Na^+ currents recorded in the whole-cell configuration in the control conditions (control) and during the 10-µM SKF 38393 treatment (10 µM SKF 38393) are shown. (b) The average current-voltage relationship of the normalised Na^+ currents before (n=6, open circles), during the 10-µM SKF 38393 (n=6, filled circles) treatment and after washout (n=4, open triangles) is shown. Na^+ currents were induced by 17 depolarisation steps that lasted 48.5 ms and were administered in 5-mV increments, every 5 s. The voltage steps were preceded by a −100-mV hyperpolarisation pre-pulse that lasted 783 ms. The holding membrane potential was −65 mV (inset in a); horizontal axis – the value of the step depolarisations and vertical axis – normalised current.

SKF 38393 (111.6 ± 13.4%, n=7, Wilcoxon test, P=0.578, Fig. 3C). Therefore, the PKA inhibitor abolished the effect of $D_{1/5}$ receptor activation on the voltage-dependent fast-inactivating Na^+ currents recorded in the cell-attached configuration in the mPFC pyramidal neurons in slices.

Control of the fast-inactivating Na^+ currents recorded in the whole-cell configuration by $D_{1/5}$ dopamine receptors

Other studies (Cantrell et al. 1999, Maurice et al. 2001, Peterson et al. 2006) demonstrated that treatment of the mPFC pyramidal neurons with a $D_{1/5}$ dopamine receptor agonist decreased the maximum amplitude of the fast-inactivating Na^+ current without affecting the Na^+ current-voltage relationship in young and young adult rats. Our study has shown that the application of a $D_{1/5}$ dopamine receptor agonist shifted the current-voltage relationship of this Na^+ current towards hyperpolarisation without changing the Na^+ current amplitude in adult rats (>60 days old). To exclude the possibility that the inhibitory effect of the $D_{1/5}$ dopamine receptor agonist on Na^+ currents was age-dependent, we recorded the fast-inactivating Na^+ current in the whole-cell configuration from freshly dispersed mPFC pyramidal neurons that were obtained from adult rats.

To stimulate the Na^+ current, the membrane potential was depolarised by rectangular voltage steps lasting 48.5 ms and conducted in 5-mV increments every 5 seconds. The voltage steps were preceded by a hyperpolarisation pre-pulse of −100 mV that lasted 783 ms. The holding membrane potential was −65 mV (inset to Figure 3Da). These voltage steps induced fast-inactivating inward Na^+ currents (Fig. 3Da). Treating neurons with 10 μM SKF 38393 decreased the Na^+ current amplitude (Fig. 3Da – control *versus* 3Da – 10 μM SKF 38393) similarly as in pyramidal neurons obtained from younger rats (Maurice et al. 2001, Peterson et al. 2006, Cantrell et al. 1999). The mean maximum current amplitude significantly decreased from 100% (control) to 76.63 ± 6.76% (P<0.001) during the 10 μM SKF38393 treatment and recovered after the washout period (93.34 ± 2.13, n=11, Friedman Test, Fr=15.8 followed by the Dunn test). The normalised Na^+ current amplitudes recorded before (n=6), during the SKF 38393 treatment (n=6) and after washout (n=4) completely overlapped (Fig. 3 Db), thus indicating that there was no shift of a current-voltage relationship in either direction. Therefore, $D_{1/5}$ dopamine receptor activation decreased the Na^+ current amplitude and did not affect the Na^+ current-voltage relationship when the recordings were performed in the whole- cell configuration from dispersed pyramidal neurons obtained from adult rats.

DISCUSSION

This study was performed on mPFC pyramidal neurons obtained from adult rats. It demonstrated that $D_{1/5}$-type receptor activation shifted the current-voltage relationship of the fast-inactivating Na^+ currents towards hyperpolarisation when recordings were performed on neurons in slices in the cell-attached configuration. The maximum amplitude of the current did not change. The cAMP/kinase A transduction system was involved. When recordings were performed from freshly dispersed mPFC pyramidal neurons in the whole-cell configuration, activation of the $D_{1/5}$ dopamine receptors decreased the fast-inactivating Na^+ current amplitude without changing the current-voltage relationship.

Effects of a dopamine receptor agonist on the membrane potential

The Na^+ currents recorded in this study were voltage-dependent. Therefore, any change in the membrane potential induced by the dopamine receptor agonist could alter the kinetic properties of these currents. It is expected that hyperpolarisation removes steady-state inactivation of the Na^+ currents and thus increases their amplitude. Furthermore, depolarisation should reinforce the steady-state inactivation and decrease the current amplitude. When current recordings are obtained in the cell-attached configuration, as in this study, the membrane potential cannot be monitored while treating the cells with the dopamine receptor agonist. Therefore, the effect of $D_{1/5}$ receptor activation on membrane potential was first investigated by using the perforated-patch method (Akaike and Harata 1994). The results from this experiment showed that the membrane potential did not change during the dopamine receptor agonist treatment; therefore, any change in the voltage-dependent and fast-inactivating Na^+ currents observed in adult rat neurons should result from the intracellular transduction that conveys information from the dopamine receptors to the Na^+ channels.

Elimination of capacitance transients in cell-attached configuration recordings

In addition to the Na^+ current, a step-wise depolarisation of the patch membrane induces a marked capacitance current when the recordings are obtained in the cell-attached configuration. Different methods were used to eliminate these Na^+-independent currents. Occasionally, voltage steps do not induce the Na^+ current and only produce the capacitance current. This "empty" trace can be subtracted from a trace with an Na^+ current in order to isolate it (Alzheimer et al. 1993, Magee and Johnston 1995). Frequently, a scaled trace generated using small voltage steps that do not induce the Na^+ current is subtracted from a trace with an Na^+ current (Gasparini and Magee 2002, Rosenkranz and Johnston 2007). In this study we produced empty traces by applying long depolarising pre-pulses to approximately −5 mV before inducing the Na^+ current with our voltage step procedure. The depolarising pre-pulse used in this study sufficiently steady-state inactivated the fast-activating and fast-inactivating Na^+ currents recorded in the whole-cell configuration (Maurice et al. 2001, Rola et al. 2002, Szulczyk and Szulczyk 2003, Rola and Szulczyk 2004, Witkowski and Szulczyk 2006) and in the cell-attached configuration (Gasparini and Magee 2002, Magee and Johnston 1995, see also Fig. 1Cb and Fig. 1Db). The amplitudes of the recorded patch Na^+ currents were similar regardless of the method used to isolate the Na^+ current (compare Magee and Johnston 1995, Astman et al. 2006).

Fast-inactivating (transient) and persistent voltage-dependent Na^+ currents recorded in cell-attached configuration

The voltage-dependent Na^+ currents in the cortical pyramidal neurons have two components: the fast-inactivating Na^+ current and the persistent Na^+ current. It is unknown whether these currents are produced by two different channels (Maurice et al. 2001) or by the same Na^+ channel (Alzheimer et al. 1993). The possible involvement of a persistent component of the Na^+ current recorded in the cell-attached configuration was excluded in our study for the following reasons: (1) It has been proposed that the pyramidal neurons in layer V of the neocortex, the persistent component of the Na^+ current is only generated by axonal Na^+ channels (Astman et al. 2006). In this study only somatic Na^+ currents were recorded. (2) The persistent component of the Na^+ current is not inactivated during prolonged voltage steps (Mantegazza et al. 2005). In this study, we subtracted the current traces induced by voltage steps preceded by depolarising pre-pulses from traces induced by voltage steps preceded by hyperpolarising pre-pulses to isolate the voltage-dependent fast-activating and fast-inactivating Na^+ currents. Therefore, any existing non-inactivating Na^+ currents should have been eliminated during this calculation. (3) According to our recordings the Na^+ currents were completely time-dependently inactivated during the voltage step, which suggests that only the transient component of the Na^+ current was recorded.

Effect of a $D_{1/5}$ agonist on the fast-inactivating Na^+ current

The results of this study indicate that activation of the $D_{1/5}$ dopamine receptors shifted the Na^+ current-voltage relationship towards hyperpolarisation when recordings were performed in the cell-attached configuration from the mPFC pyramidal neurons in slices obtained from adult rats. Previous studies demonstrated that the Na^+ current amplitude decreased without a current-voltage relation shift in response to the $D_{1/5}$ dopamine agonist. These studies were performed in the whole-cell configuration, on dispersed mPFC pyramidal neurons obtained from younger rats (Maurice et al. 2001, Peterson et al. 2006).

To exclude the possibility that different results were caused by the different ages of the animals, we tested the effect of $D_{1/5}$ dopamine receptor activation on Na^+ currents recorded in the whole-cell configuration from dispersed pyramidal neurons obtained from adult animals. We showed that the Na^+ current amplitude decreased and that the current-voltage relationship did not change during $D_{1/5}$ receptor activation, exactly as in the pyramidal neurons obtained from younger animals (Maurice et al. 2001, Peterson et al. 2006). Therefore, in pyramidal neurons obtained from adult rats the effect of the $D_{1/5}$ dopamine receptors on the fast- inactivating Na^+ current depended on the current recording method.

A similar discrepancy was also found in previous studies that investigated fast-inactivating Na^+ currents in cardiac myocytes. When recordings were performed in the whole-cell configuration, the amplitude of the Na^+ currents decreased (Ono et al. 1989, Schubert et al.

1990). When recordings were obtained in the cell-attached configuration, however, there was a negative shift in the current-voltage relationship and the current amplitude did not change (Ono et al. 1993).

Several factors could be responsible for the different effects of the $D_{1/5}$ dopamine receptors on the fast-inactivating Na^+ currents when they are recorded in the whole-cell configuration rather than in the cell-attached configuration. During preparation of dissociated neurons for recording of the Na^+ currents in the whole-cell configuration, the cells undergo enzymatic digestion and their branches are truncated. It has been shown that the kinetic properties of fast-inactivating Na^+ currents are significantly altered in cells treated with proteolytic enzymes (Bezanilla and Armstrong 1977, Berra-Romani et al. 2005). In the cell-attached configuration, i.e. opposite to the whole-cell configuration, the intracellular environment was preserved. Dopamine receptors are G-protein-coupled receptors that control intracellular effectors through intracellular transduction pathways. Previous studies have shown that intracellular transduction pathways are altered when current recordings are obtained in the whole-cell configuration (Akaike and Harata 1994).

CONCLUSIONS

This study indicates that $D_{1/5}$ dopamine receptor stimulation evokes a negative shift in the current-voltage relationship of the fast-inactivating Na^+ current without changing the maximum current amplitude. This results in a decrease of the Na^+ current voltage threshold and increase in the Na^+ current availability in response to suprathreshold stimulation. Therefore, during $D_{1/5}$ dopamine receptor stimulation fast-inactivating Na^+ currents support mPFC pyramidal neuron activity just as other pyramidal neuron effectors: NMDA receptors which are upregulated (Chen et al. 2004, Gonzalez-Islas and Hablitz 2003, Kruse et al. 2009, Seamans et al. 2001, Tseng and O'Donnell 2005), voltage-dependent Ca^{++} currents (Heng et al. 2011) and persistent Na^+ currents (Gorelova and Yang 2000, Maurice et al. 2001) which are increased, and voltage-dependent ID-type K^+ currents which are supressed (Dong and White 2003). In all of these studies, with the exception of the persistent Na^+ currents, the cAMP/kinase A system was involved in the signal transduction pathway from the $D_{1/5}$ receptor to the Na^+ channels. In our study the effects of the $D_{1/5}$ dopamine receptors on fast-inactivating Na^+ currents recorded in the cell-attached configuration also depended on the cAMP/kinase A transduction system. The persistent Na^+ currents analysed in other studies were not affected by the cAMP/kinase A system (Maurice et al. 2001) or increased in a kinase C-dependent manner (Gorelova and Yang 2000).

The enhancement of voltage-dependent Na^+ channel current by $D_{1/5}$ dopamine receptors may be one of the factors responsible for increasing the excitability of prefrontal cortical pyramidal neurons, the activation of which is believed to be representative of the working memory process (Goldman-Rakic 1995, Sobotka et al. 2005). This mechanism also implies that Na^+ channel inhibitors should impair working memory. Na^+ channel inhibitors are commonly used in treatments for epilepsy and neuralgia, and impaired working memory has been shown to be an important and principal side effect of anticonvulsive medications. The most severe cases of impaired working memory occur in epileptic patients given Na^+ channel inhibitors, as shown by comparisons with epileptic patients treated with other types of medications (Helmstaedter et al. 2010, Sommer and Fenn 2010) and healthy volunteers (Meador et al. 2007).

ACKNOWLEDGEMENTS

We would like to thank Marta Kuzniarska and Izabela Zaborowska for their technical assistance. This study was supported by grant no. NCN/MNiSzW- N N401 030037.

REFERENCES

Akaike N, Harata N (1994) Nystatin perforated patch recording and its applications to analyses of intracellular mechanisms. Jpn J Physiol 106: 433–473.

Alzheimer C, Schwindt PC, Crill, WE (1993) Modal gating of Na+ channels as a mechanism of persistent Na+ current in pyramidal neurons from rat and cat sensorimotor cortex. J Neurosci 13: 660–673.

Astman N, Gutnick MJ, Fleidervish IA (2006) Persistent Sodium Current in Layer 5 Neocortical neurons is primarily generated in the proximal axon. J Neurosci 26: 3465–3473.

Baddeley AD, Hitch GJ (1974) Working memory. In: The psychology of Learning and Motivation (Bower GA, Ed.). Acadaemic Press, San Diego, CA. p. 47–89.

Beaulieu JM, Gainetdinov RR (2011) The physiology, signaling, and pharmacology of dopamine receptors. Pharmacol Rev 63: 182–217.

Berger B, Gaspar P, Verney C (1991) Dopaminergic innervation of the cerebral cortex: unexpected differences between rodents and primates. Trends Neurosci 14: 21–27.

Berra-Romani R, Blaustein MP, Matteson DR (2005) TTX-sensitive voltage-gated Na^+ channels are expressed in mesenteric artery smooth muscle cells. Am J Physiol Heart Circ Physiol 289: 137–145.

Bezanilla F, Armstrong CM (1977) Inactivation of the sodium channel. II. Gating current experiments. J Gen Physiol 70: 549–566.

Cantrell AR, Scheuer T, Catterall WA (1999) Voltage-dependent neuromodulation of Na+ channels by D1-like dopamine receptors in rat hippocampal neurons. J Neurosci 19: 5301–5310.

Carr DB, Day M, Cantrell AR, Held J, Scheuer T, Catterall WA, Surmeier DJ (2003) Transmitter modulation of slow, activity-dependent alterations in sodium channel availability endows neurons with a novel form of cellular plasticity. Neuron 39: 793–806.

Chen G, Greengard P, Yan Z (2004) Potentiation of NMDA receptor currents by dopamine D_1 receptors in prefrontal cortex. Proc Natl Acad Sci U S A 101:2596–2600.

Chen L, Bohanick JD, Nishihara M, Seamans JK, Yang CR (2007) Dopamine D1/5 receptor-mediated long-term potentiation of intrinsic excitability in rat prefrontal cortical neurons: Ca^{2+}-dependent intracellular signaling. J Neurophysiol 97: 2448-2464.

Crill WE (1996) Persistent sodium current in mammalian central neurons. Annu Rev Physiol 58: 349–362.

Dash P, Moore A, Kobori N, Runyan J (2007) Molecular activity underlying working memory. Learn Mem 14: 554–563.

Dong Y, White FJ (2003) Dopamine D1-class receptors selectively modulate a slowly inactivating potassium current in rat medial prefrontal cortex pyramidal neurons. J Neurosci 23: 2686–2695.

Gasparini S, Magee JC (2002) Phosphorylation-dependent differences in the activation properties of distal and proximal dendritic Na^+ channels in rat CA1 hippocampal neurons. J Physiol 541: 665–672.

Goldman-Rakic PS (1995) Cellular basis of working memory. Neuron 14: 477–485.

Gonzalez-Islas C, Hablitz JJ (2003) Dopamine enhances EPSCs in layer II-III pyramidal neurons in rat prefrontal cortex. J Neurosci 23: 867–875.

Gorelova NA, Yang CR (2000) Dopamine D1/D5 receptor activation modulates a persistent sodium current in rat prefrontal cortical neurons in vitro. J Neurophysiol 84: 75–87.

Helmstaedter C, Schoof K, Rossmann T, Reuner G, Karlmeier A, Kurlemann G (2010) Introduction and first validation of EpiTrack Junior, a screening tool for the assessment of cognitive side effects of antiepileptic medication on attention and executive functions in children and adolescents with epilepsy. Epilepsy Behav 19: 55–64.

Heng LJ, Markham JA, Hu XT, Tseng KY (2011) Concurrent upregulation of postsynaptic L-type Ca(2+) channel function and protein kinase A signaling is required for the periadolescent facilitation of Ca(2+) plateau potentials and dopamine D1 receptor modulation in the prefrontal cortex. Neuropharmacology 60: 953–962.

Henze DA, González-Burgos GR, Urban NN, Lewis DA, Barrionuevo G (2000) Dopamine increases excitability of pyramidal neurons in primate prefrontal cortex. J Neurophysiol 84: 2799–2809.

Holz GG, Kang G, Harbeck M, Roe MW, Chepurny OG (2006) Cell physiology of cAMP sensor Epac. J Physiol 577: 5–15.

Isaac JT, Wheal HV (1993) The local unaesthetic QX-314 enables enhanced whole-cell recordings of excitatory synaptic currents in rat hippocampal slices in vitro. Neurosci Lett 150: 227–230.

Kolb B (1984) Functions of the frontal cortex of the rat: a comparative review. Brain Res 320: 65–98.

Kruse MS, Premont J, Krebs MO, Jay TM, (2009) Interaction of dopamine D1 with NMDA NR1 receptors in rat prefrontal cortex. Eur Neuropsychopharmacol 19: 296–304.

Lavin A, Grace AA (2001) Stimulation of D1-type dopamine receptors enhances excitability in prefrontal cortical pyramidal neurons in a state-dependent manner. Neuroscience 104: 335–346.

Magee JC, Johnston D (1995) Characterization of single voltage-gated Na+ and Ca2+ channels in apical dendrites of rat CA1 pyramidal neurons. J Physiol 487: 67–90.

Mantegazza M, Yu FH, Powell AJ, Clare JJ, Catterall WA, Scheuer T (2005) Molecular determinants for modulation of persistent sodium current by G-protein betagamma subunits. J Neurosci 25: 3341–3349.

Maurice N, Tkatch T, Meisler M, Sprunger LK, Surmeier DJ (2001) D_1/D_5 dopamine receptor activation differentially modulates rapidly inactivating and persistent sodium currents in prefrontal cortex pyramidal neurons. J Neurosci 21: 2268–2277.

Meador KJ, Gevins A, Loring DW, McEvoy LK, Ray PG, Smith ME, Motamedi GK, Evans BM, Baum C (2007) Neuropsychological and neurophysiologic effects of carbamazepine and levetiracetam. Neurology 69: 2076–2084.

Moore AR, Zhou WL, Potapenko ES., Kim EJ, Antic SD (2011) Brief dopaminergic stimulations produce transient physiological changes in prefrontal pyramidal neurons. Brain Res 1370: 1–15.

Nowak K, Meyza K, Nikolaev E, Hunt MJ, Kasicki S (2012) Local blockade of NMDA receptors in the rat prefrontal cortex increases c-Fos expression in multiple subcortical regions. Acta Neurobiol Exp (Wars) 72: 207–218.

Ono K, Kiosue T, Arita M (1989) Isoproterenol, DBcAMP, and forskolin inhibit cardiac sodium current. Am J Physiol Cell Physiol 256: 1131–1137.

Ono K, Fozzard HA, Hanck DA (1993) Mechanism of cAMP dependent modulation of cardiac sodium channel current kinetics. Circ Res 72: 807–815.

Penit-Soria J, Audinat E, Crepel F (1987) Excitation of rat prefrontal cortical neurons by dopamine: an in vitro electrophysiological study. Brain Res 425: 263–274.

Peterson JD, Wolf ME, White FJ (2006) Repeated amphetamine administration decreases D_1 dopamine receptor-mediated inhibition of voltage-gated sodium currents in the prefrontal cortex**.** J Neurosci 26: 3164–3168.

Rola R, Szulczyk B, Szulczyk P, Witkowski G (2002) Expression and kinetic properties of Na+ currents in rat cardiac dorsal root ganglion neurons. Brain Res 947: 67–77.

Rola R, Szulczyk P (2004) Kinetic properties of voltage-gated Na^+ currents in rat muscular sympathetic neurons with and without ATP and GTP in intracellular solution. Neurosci Lett 359: 53–56.

Rosenkranz JA, Johnston D (2007) State-dependent modulation of amygdala inputs by dopamine-induced enhancement of sodium currents in layer V enthorinal cortex. J Neurosci 27: 7054–7069.

Schubert B, Vandongen AMJ, Kirch G, Brown AM, (1990) Inhibition of cardiac Na+ currents by isoprotenerol. Am J Physiol Heart Circ Physiol 258: 977–982.

Seamans JK, Durstewitz D, Christie BR, Stevens CF, Sejnowski TJ (2001) Dopamine D1/D5 receptor modulation of excitatory synaptic inputs to layer V prefrontal cortex neurons. Proc Natl Acad Sci U S A 98: 301–306.

Shi WX, Zheng P, Liang XF, Bunney BS (1997) Characterization of dopamine-induced depolarization of prefrontal cortical neurons. Synapse 26: 415–422.

Sobotka S, Diltz MD, Ringo JL (2005) Can delay-period activity explain working memory? J Neurophysiol 93: 128–136.

Sommer BR, Fenn HH (2010) Review of topiramate for the treatment of epilepsy in elderly patients. Clin Interv Aging 5: 89–99.

Spear LP (2000) Neurobehavioral changes in adolescence. Curr Dir Psychol Sci 9: 111–114.

Szulczyk B, Szulczyk P (2003) Postdecentralization plasticity of voltage-gated Na+ currents in rat glandular sympathetic neurons. Neurosci Lett 343: 105–108.

Thurley K, Senn W, Lüscher HR (2008) Dopamine increases the gain of the input-output response of rat prefrontal pyramidal neurons. J Neurophysiol 99: 2985–2997.

Tseng KY, O'Donnell P (2004) Dopamine–glutamate interactions controlling prefrontal cortical pyramidal cell excitability involve multiple signaling mechanisms. J Neurosci 24: 5131–5139.

Tseng KY, O'Donnell P (2005) Post-pubertal emergence of prefrontal cortical up states induced by D_1–NMDA co-activation. Cereb Cortex 15: 49–57.

Williams GW, Castner SA (2006) Under the curve: critical issues for elucidating D1 receptor function in working memory. Neuroscience 139: 263–276.

Witkowski G, Szulczyk P (2006) Opioid mi receptor activation inhibits sodium currents in prefrontal cortical neurons via a protein kinase A- and C-dependent mechanism. Brain Res 1094: 92–106.

Witkowski G, Szulczyk B, Rola R, Szulczyk P (2008) D(1) dopaminergic control of G protein-dependent inward rectifier K(+) (GIRK)-like channel current in pyramidal neurons of the medial prefrontal cortex. Neuroscience 155: 53–63.

Yang CR, Seamans JK (1996) Dopamine D1 receptor actions in layers V-VI rat prefrontal cortex neurons in vitro: modulation of dendritic-somatic signal integration. J Neurosci 16: 1922–1935.

Zohar O, Rubovitch V, Milman A, Schreiber S, Pick CG (2011) Behavioral consequences of minimal traumatic brain injury in mice. Acta Neurobiol Exp (Wars) 71: 36–45.